

## AN INVESTIGATION ON STRUCTURAL AND ELECTRICAL PROPERTIES OF CLOSE-SPACED SUBLIMATION GROWN CdTe THIN FILMS IN DIFFERENT GROWTH CONDITIONS

F. M. T. ENAM<sup>a</sup>, K.S. RAHMAN<sup>a</sup>, M. I. KAMARUZZAMAN<sup>a</sup>, K. SOBAYEL<sup>a</sup>  
M. AKTHARUZZAMAN<sup>b</sup>, N. AMIN<sup>a,b\*</sup>

<sup>a</sup>*Department of Electrical, Electronic and Systems Engineering, Faculty of Engineering and Built Environment, The National University of Malaysia, 43600 Bangi, Selangor, Malaysia*

<sup>b</sup>*Solar Energy Research Institute, The National University of Malaysia, 43600 Bangi, Selangor, Malaysia*

CdTe is considered as one of the most auspicious materials as absorber layer for fabricating thin film solar cells with highest efficiency of 22.1% at present reported by First Solar Inc. Growth conditions and parameters are crucial aspects to acquire high quality and pin hole free thin absorber layer. In this study, a comparative analysis has been executed for close-spaced sublimation (CSS) grown CdTe thin films in both dynamic and static conditions. These growth conditions may have dependence on the way of inert gas flow during deposition. Deposited films have been characterized by using XRD, FESEM, AFM and Hall Effect Measurement. The XRD pattern reveals the presence of zinc-blende cubic structure with ideal orientation (111) confirming polycrystalline nature. The FESEM characterization illustrates the films that are homogenous, uniform and have less crystal defects. AFM analysis has been carried out to know the surface topography and roughness which has the increasing trend for thicker films. Moreover, the electrical parameters such as carrier concentration, mobility, resistivity, and conductivity have been measured from Hall Effect measurement.

(Received January 4, 2017; Accepted April 10, 2017)

*Keywords:* Close Spaced Sublimation, Growth Condition, CdTe thin film, XRD, AFM.

### 1. Introduction

Cadmium Telluride is the leading contender among the chalcogenide semiconductor for utilizing in large scale thin film solar cell devices [1]. For photovoltaic energy conversion, it has a direct band gap of 1.45 eV, which is nearly supreme for absorption spectrum. It has high optical absorption coefficient that absorb all energy incident radiation with above its bandgap within the range of 1-2  $\mu\text{m}$  from the surface [2-5]. Moreover 90% of obtainable photons have been absorbed by CdTe [6-7]. Numerous deposition techniques are employed to fabricate effective heterojunction CdTe solar cells such as sputter deposition, chemical bath deposition (CBD), high vacuum evaporation and close-spaced sublimation (CSS), etc. Close spaced sublimation (CSS) is one of the popular technologies for large scale CdTe manufacturing due to its high throughput [8-13]. The CSS technique is very attractive for CdTe thin film deposition as it offers high deposition rates and can be minimally scaled up for manufacturing intentions. The significant process parameters for CSS system are the pressure in the reaction tube, sublimation time, the nature of the atmosphere, the composition of the source material and the temperatures of the source and the substrate. These parameters are inter-related. To find the deposition rate, the partial pressure of Cd and Te<sub>2</sub> in the reaction tube is vital. The sublimation rate enhances swiftly at a given source temperature as the pressure in the reaction tube is lessened from the atmospheric pressure.

---

\*Corresponding author: nowshad@ukm.edu.my

In case of fixed source-substrate spacing, high thermal conductivity of the ambient gas tends to increase the substrate temperature, thus reducing the growth rate. At too-low pressures, the mean free path of the gaseous species in the reaction tube raises, and the condensation process is no longer restricted to the space between the substrate and the source material [14-18]. The effect of the nature of the ambient gas is related mainly to its thermal conductivity. Apart from temperature and time, the flow of inert gas in dynamic and static modes is really noteworthy in the growth of high quality CdTe thin film. In dynamic condition, the CSS chamber has been kept in vacuum by continuous flow of inert gas (Ar) from the closed chamber to the vacuum pump. On the other hand, in static mode, certain working pressure of inert gas remained in the chamber while the vacuum is off confirming no inert gas flow from close chamber to the vacuum pump. Therefore, the main purpose of this study is to investigate the influence of different growth conditions on the structural and electrical properties of CSS grown CdTe thin films for photovoltaic application.

## 2. Experimental

CdTe thin films were deposited on borosilicate glass substrates of 3 cm × 3 cm via Close-Spaced Sublimation (CSS) method. All substrates have been cleaned by ultrasonic bath process by a sequence of methanol → acetone → methanol → deionized water and finally dried by N<sub>2</sub> gas flow. The source material has been used in this study is 5N CdTe (99.99%) powder which has been sintered at 700°C for 30 min. In sintering, the empty space of the bottom susceptor, which is made by graphite, has been filled up by CdTe powder properly. Then the powder is heated at specific pressure and temperature to make it solid and compact. The growth of CdTe films are carried out in a simple reactor, schematic of which is shown in Fig. 1.

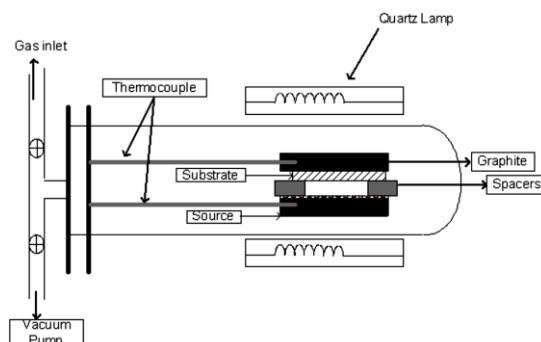


Fig. 1: Schematic diagram of Close-Spaced Sublimation (CSS) apparatus

Borosilicate spacers (1 cm x 1 cm) were used to separate the substrate from the source. For monitoring and controlling the temperature, thermocouples were inserted in to the graphite plates (susceptor). These plates were heated by two 2 KW tungsten halogen lamps independently. Gas inlet and outlet ports were used to control the ambience of the chamber. CdTe films were grown in a stationary ambient. Spacing between source and substrate was kept constant at 2 mm for CdTe depositions in both dynamic and static conditions.

Table 1: Deposition Conditions used in the CSS Growth of CdTe Films

Substrate Temperature	580-600°C
Source Temperature	620-640°C
Working Pressure	1.5-2.0 Torr (Ar gas atmosphere)
Spacing	1-2 mm
Deposition Time	5 min

Before starting deposition, chamber was kept in vacuum. After that pure N<sub>2</sub> and Ar gas were utilized for purging and deposition, respectively. Pure N<sub>2</sub> was also used for venting the chamber. 1.8 Torr Ar gas pressure is appropriate for CdTe thin film deposition. During dynamic condition growth of CdTe, the Ar gas flows from inlet and evacuates from outlet ports continuously. In static condition, Ar gas remained constant at certain pressure in a closed chamber without any flow. The substrate temperature is varied in the range of 580-600°C while the source temperature is varied in the range of 620-640°C. By keeping other deposition parameters constant, the growth condition is changed. The chamber is evacuated several times and then is kept at 1.8 Torr of Ar gas to create the appropriate atmosphere for deposition.

### 3. Result and discussions

#### 3.1 Structural Properties of CdTe Thin Films

To examine the crystallographic structure, the close-spaced sublimation (CSS) grown CdTe thin films has been characterized and evaluated through X-ray powder diffraction (XRD) data taken by 'BRUKER aXS-D8 Advance Cu-K $\alpha$ ' diffractometer. II-VI chalcogenide semiconductor materials illustrate the dual structure and they can be formed as either cubic (zinc blende) or hexagonal (wurtzite) crystal structures. The lattice parameter 'a' for cubic phase structure [hkl] for the films has been calculated from the Brag's law and Vegard's law [19].

$$d(hkl) = (\lambda/2)\text{cosec}\theta \quad (1)$$

$$a_{\text{cubic}} = d_{\text{hkl}} (h^2+k^2+l^2)^{1/2} \quad (2)$$

Where d is the interspacing in the atomic lattice between the planes,  $\lambda$  is the X-ray wavelength (0.15406 nm),  $\theta$  is the angle between the incident ray and scattering planes and a is the lattice constant. The mean crystallite sizes (D) of the films are intended via Scherrer formula [20].

$$D(hkl) = 0.9\lambda/\beta\cos\theta \quad (3)$$

Where  $\theta$  is the Bragg diffraction angle,  $\lambda$  is the X-ray wavelength (0.15406 nm) and  $\beta$  is the full width at half maximum [FWHM] of the film diffraction peak at  $2\theta$ . FWHM values are correlated with the crystallinity. The higher values of FWHM points out the decline of the films crystallinity, whereas the bigger crystallite sizes stipulate the improved crystallinity of the films. The developed microstrain ( $\varepsilon$ ) has been deducted from the following relation [21-22].

$$\varepsilon = \beta/4\tan\theta \quad (4)$$

Here,  $\beta$  and  $\theta$  has their usual significances. By utilizing Williamson and Smallman's relation [23-24], the dislocation density of thin films is calculated.

$$\delta = n/D^2 \quad (5)$$

Here, n is a factor, which is regarded as approximately identical to unity for minimum dislocation density and D is the crystallite size or grain size.

From Fig. 2, it is clear that the films grown from CSS process in both dynamic and static condition exhibit crystalline nature with a preferential orientation along the (111)<sup>cub</sup> plane found at  $2\theta=23.8^\circ$  confirming a pure cubic zinc blende structure. Another two low intensity peaks were found along the (220)<sup>cub</sup> and (311)<sup>cub</sup> orientation around  $2\theta=39.31^\circ$  and around  $2\theta=46.51^\circ$ , respectively. Crystallinity is higher in static condition than dynamic condition for CdTe thin film. All the diffraction peaks are well matched with the JCPDS (00-015-0770) file and are in good agreement with the literature of CdTe cubic structure [25-28].

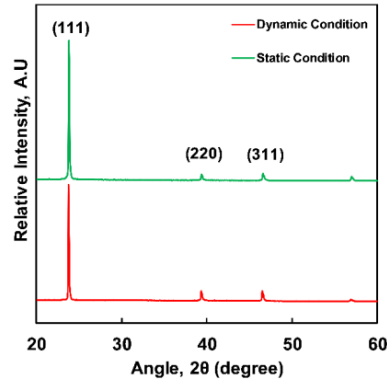


Fig. 2: XRD Spectra of deposited CdTe in Dynamic and Static condition

Table 2: Calculated values of the crystallographic parameters of CSS grown CdTe thin films in different growth conditions

Deposited Sample	hkl	$d_{hkl}$ (nm)	a (nm)	$\beta$ (deg)	$D_{hkl}$ (nm)	$\epsilon$ [ $\times 10^{-3}$ ]	$\delta$ [ $\times 10^{11}$ ]( $\text{cm}^{-2}$ )
CdTe grown in dynamic condition	(111)	0.36	0.63	1.4	5.80	0.028	0.029
	(220)	0.23	0.64	0.5	12.07	0.008	0.006
	(311)	0.19	0.64	0.7	17.31	0.005	0.003
CdTe grown in static condition	(111)	0.36	0.63	1.8	4.5	0.035	0.0489
	(220)	0.23	0.64	0.9	9.4	0.010	0.011
	(311)	0.19	0.64	0.7	12.4	0.007	0.006

From the calculated values above the average crystallite sizes are in the range of 5 nm–18 nm. From Table 2, it is observed that the highest crystallite size (17.31) is found for the (311)<sup>cube</sup> phase whereas the (111)<sup>cube</sup> phase shows lowest value of crystallite size for deposited CdTe thin film in dynamic condition. The lattice constant is found 0.64 nm in both conditions for all CdTe diffracted peaks. The highest micro-strain of  $0.035 \times 10^{-3}$  is obtained for (111)<sup>cube</sup> phase for grown CdTe in static condition which indicates the highest lattice misfit and dislocation in the film structure. The maximum value of dislocation density  $0.049 \times 10^{11}$  is also found for the same films.

### 3.2 Surface Morphology of CdTe Thin Films

Field Emission Scanning Electron Microscopy (FESEM) images have been taken for 20  $\mu\text{m}$  thin CdTe layer to investigate the surface morphology and 5  $\mu\text{m}$  for the cross-sectional view. Fig. 3 shows FESEM images of CdTe deposited in both dynamic and static conditions. From the micrographs, it is observed that the CdTe thin film grown in dynamic condition is less compact and grain size is much smaller compared to the films grown in static condition. In static condition, the grain seems very large, smooth, sharp and pin hole free. The deposition rate and the thickness are higher for CSS grown CdTe thin films in static condition. From the figure, it is clearly visible that the thickness of CdTe in dynamic condition is 2.78  $\mu\text{m}$  which is less than the thickness of 4.09  $\mu\text{m}$  for CdTe thin film in static condition. Dynamic condition may have inhibited the proper sublimation of CdTe films, which have caused less amount of CdTe deposition on substrate. Hence, there is crucial need to optimize CdTe growth condition to get the larger grain as well as deposition as thickness. The images also illustrate that the surface morphology and the average grain size of the films are strongly dependent on the CdTe growth condition.

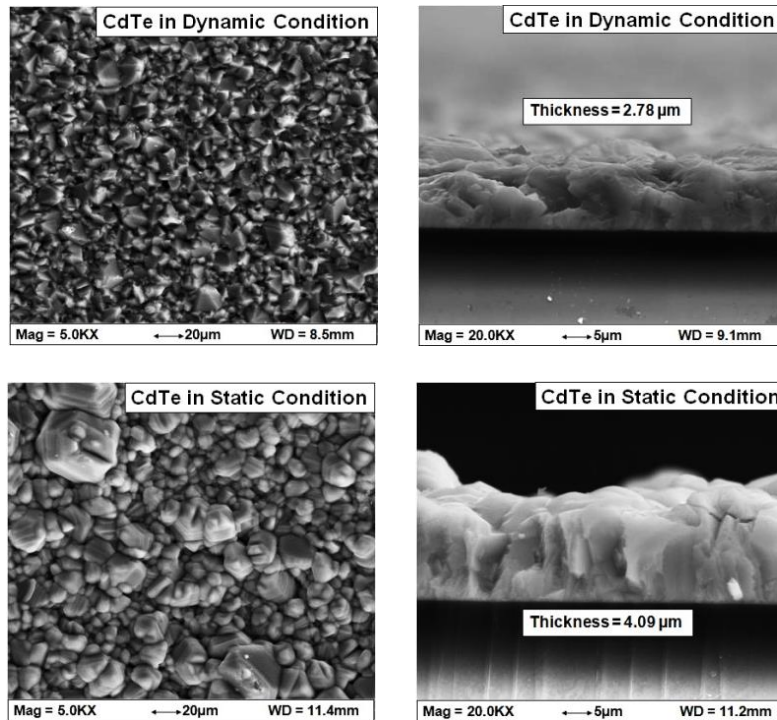


Fig. 3: FESEM surface morphology and cross section FESEM thickness images of CSS deposited CdTe thin films

### 3.3 Surface Topography of CdTe Thin Films

Atomic Force Microscopy (AFM) is basically employed for exploring the surface texturing of the films. Investigation of the surface topography and roughness of CSS grown CdTe thin films was analyzed by “NANOSURF EASYSCAN 2 AFM” (Atomic Force Microscopy) SYSTEM”. Average roughness ( $S_a$ ) and RMS roughness ( $S_q$ ) values are achieved for CSS grown CdTe thin film in both dynamic and static conditions which is shown in Fig. 4.

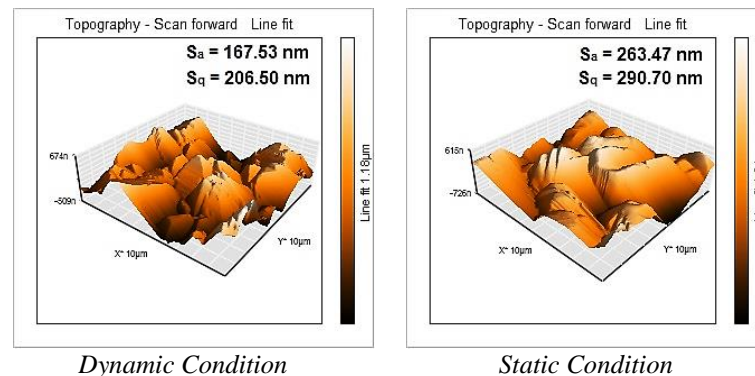


Fig. 4: 3D AFM images for showing roughness values of CSS deposited CdTe thin films

In dynamic condition, the average and root mean square (RMS) of the roughness were about 167.53 nm and 206.50 nm, respectively. When deposition condition is changed to static, the average and root mean square value of the roughness increased to 263.47 nm and 290.70 nm, respectively. From the topography images, it is visible that the surface roughness was strongly affected by growth conditions. Therefore, it is essential to choose the proper growth condition for high quality CdTe thin films.

### 3.4 Electrical Properties of CdTe Thin Films

The electrical properties of the CdTe thin films prepared by CSS in various growth conditions have been investigated by Hall-Effect measurements with an integrated resistivity/Hall measurement system (ECOPIA 3000). The measurements were carried out at room temperature.

*Table 3: Electrical parameters of deposited CdTe thin films in different growth conditions*

Sample	Bulk Concentration (/cm <sup>3</sup> )	Mobility (cm <sup>2</sup> /Vs)	Resistivity (Ω-cm)
CdTe in Dynamic Condition	3.518x10 <sup>11</sup>	1.283	1.384x10 <sup>05</sup>
CdTe in Static Condition	3.897x10 <sup>14</sup>	5.982	2.677x10 <sup>04</sup>

From the table, it is seen that the bulk carrier concentration is higher for films grown in static condition. Therefore, the highest mobility (5.982 cm<sup>2</sup>/Vs) and lowest resistivity (2.677×10<sup>4</sup> Ω-cm) was obtained in static condition for CdTe thin film. It was also evident that bulk concentration of the films was in the order of 10<sup>14</sup> cm<sup>-3</sup> which was maximum (3.897×10<sup>14</sup> /cm<sup>3</sup>) for static condition and also greater than the film grown in dynamic condition. It is found that better crystallinity and higher carrier concentration results in lower electrical resistivity, which is observed from this study. This happens mainly due to reduced carrier scattering and recombination across the grain boundaries.

## 4. Conclusions

The structural, morphological, topographical and electrical properties of CdTe thin films grown by both dynamic and static condition have been investigated elaborately by XRD, FESEM, AFM and Hall-effect measurement analysis. The XRD reveals that the CdTe absorber layer, in both conditions, shows cubic crystallinity with (111)<sup>cube</sup> preferential orientation around 2θ=23.8°, where the diffraction peak intensity is higher in static mode. From FESEM, it is visible that CdTe grown films in dynamic condition have more pinholes and less grain size comparing to static condition. For dynamic condition, the average and root mean square (RMS) roughness of CdTe film are lower than that in the static mode. The highest mobility was obtained for the CdTe thin films deposited by CSS in static condition with the lowest resistivity. Therefore, it can be concluded that in order to get higher quality thin film as absorber layer for CdTe solar cells, the deposited thin films by close-spaced sublimation (CSS) process in static condition are preferable than in dynamic condition.

## Acknowledgment

The authors would like to acknowledge and appreciate the contribution of The National University of Malaysia through the research grant with code DIP-2015-021 and GUP-2016-042 and The Solar Energy Research Institute of The National University of Malaysia for the grant with code AP-2015-003.

## References

- [1] G.G. Rusu, Journal of Optoelectronics and Advanced Materials, **3**, 4, 861-866 (2001).

- [2] C.S. Ferekides, D. Marinskiy, V. Viswanathan, B. Tetali, V. Palekis, P. Selvaraj, D.L. Morel, *Thin Solid Films*, **361-362** (2000).
- [3] T.L. Chu, S.S. Chu, *Progress in Photovoltaics: Research and Applications*, **1(1)**, 31-42 (1993).
- [4] T.L. Chu, S.S. Chu, J. Britt, G. Chen, C. Ferekides, N. Schultz, C. Wang & C. Wu, *Photovoltaic advanced research and development project*, **268**, 88-93 (1992).
- [5] J. Schaffner, M. Motzko, A. Tueschen, A. Swirschuk, H.J. Schimper, A. Klein, T. Modes, O. Zywitzki and W. Jaegermann, *Journal of Applied Physics*, **110**, 064508 (2011).
- [6] B.McCandless, R.Birkmire, *Solar Cell*, **31**, 527 (1990).
- [7] P.V. Meyers, C.H. Liu, T.J. Frey, U.S. Patent **4(710)**,589 (1987).
- [8] R.W. Birkmire, B.E. McCandless, S.S. Hegedus, *Int. J. Sol. Energy*, **12**, 145 (1992).
- [9] S. Lalitha, R. Sathyamoorthy, S. Senthilarasu, A. Subbarayan, *Solar Energy Materials and Solar Cells*, **90**, 694 (2006).
- [10] N. Bakr, *J. Cryst. Growth*, **235**, 217 (2002).
- [11] R. Sathyamoorthy, S. Narayandass, D. Mangalaraj, *Solar Energy Mater. Solar Cells*, **76**, 217 (2003).
- [12] X. Mathew, N. Mathews, P. Sebastian, C. Flores, *Solar Energy Mater. Solar Cells*, **81**, 397 (2004).
- [13] S. Ringel, A. Smith, M. MacDougall, A. Rohatgi, *J. Appl. Phys*, **70**, 881 (1991).
- [14] T. Chu, S. Chu, C. Ferekides, J. Britt, C. Wu, *J. Appl. Phys*, **71**,3870 (1992).
- [15] G. Hernandez, X. Mathew, J. Enraquez, B. Morales, M. Lira, J. Toledo, A. Juarez, J. Campos, *J. Mater. Sci*, **39**,1515 (2004).
- [16] A. Nakano, S. Ikegami, H. Matsumoto, H. Uda, Y. Komatsu, *Solar Cells*, **17**, 233 (1986).
- [17] S. Lalitha, S.Zh. Karazhanovb, P. Ravindran, S. Senthilarasu, R. Sathyamoorthy, J. Janabergenov, *Physics B*, **387**, 227 (2007).
- [18] Sukhvir Singh, Rajeev Kumar, K.N. Sood, *Thin Solid Films*, **519**, 1078 (2010).
- [19] M.A. Islam, M.S. Hossain, M.M. Aliyu, J. Husna, M.R. Karim, K. Sopian, N. Amin, 38<sup>th</sup> PVSC, 000151-000155 (2012).
- [20] M.A. Islam, Q. Huda, M.S. Hossain, M.M. Aliyu, M.R. Karim, K. Sopian, N. Amin, *Current Applied Physics*, **13**, 115-121 (2013).
- [21] J.C. Osuwa, C.I. Oriaku, I.A. Kalu, *Chalcogenide Letters*, **6**, 433-436 (1970).
- [22] B. E. Warren, *X-ray Diffraction*, Dover publications, New York, 1990.
- [23] M. A. Islam, Q. Huda, M.S. Hossain, M. M. Aliyu, M. R. Karim, K. Sopian, N. Amin, *Current Applied Physics*, **13**, S115 (2013).
- [24] D. H. Hwang, J. H. Ahn, K. N. Hui, K. S. Hui and Y. G. Son, *Nanoscale Res Lett*, pp. 26,2012.
- [25] M. A. Islam, M. S. Hossain, M. M. Aliyu, Y. Sulaiman, M. R. Karim, K. Sopian, N. Amin, 7<sup>th</sup> International Conference on Electrical and Computer Engineering, Dhaka, Bangladesh, 2012.
- [26] K. Sarmah, R. Sarma, H. L. Das, *Chalcogenide Letters*, **5(8)**, 153 (2008).
- [27] M.A. Islam, M.S. Hossain, M. M. Aliyu, J. Husna, M. R. Karim, K. Sopian, N. Amin, 38<sup>th</sup> PVSC, Austin, USA, 2012.
- [28] M.A. Islam, Q. Huda, M.S. Hossain, M.M. Aliyu, M.R. Karim, K. Sopian, N. Amin, *Current Applied Physics*, **13**, 115 (2013).